

Supporting information for Acidity and Phase Behavior of Frozen Hydrochloric Acid during Thawing

Radim Štůsek¹⁾, Lukáš Veselý¹⁾, Markéta Melicharová¹⁾, Jan Zezula¹⁾, Johannes Giebelmann²⁾, Thomas Loerting²⁾, Dominik Heger^{1)}*

¹⁾Department of Chemistry, Faculty of Science, Masaryk University, Kamenice 5, 625 00 Brno, Czech Republic

²⁾Institute of Physical Chemistry, University of Innsbruck, 6020 Innsbruck, Austria

*Dominik Heger

Email: hegerd@chemi.muni.cz

Phone: +420 549 49 3322

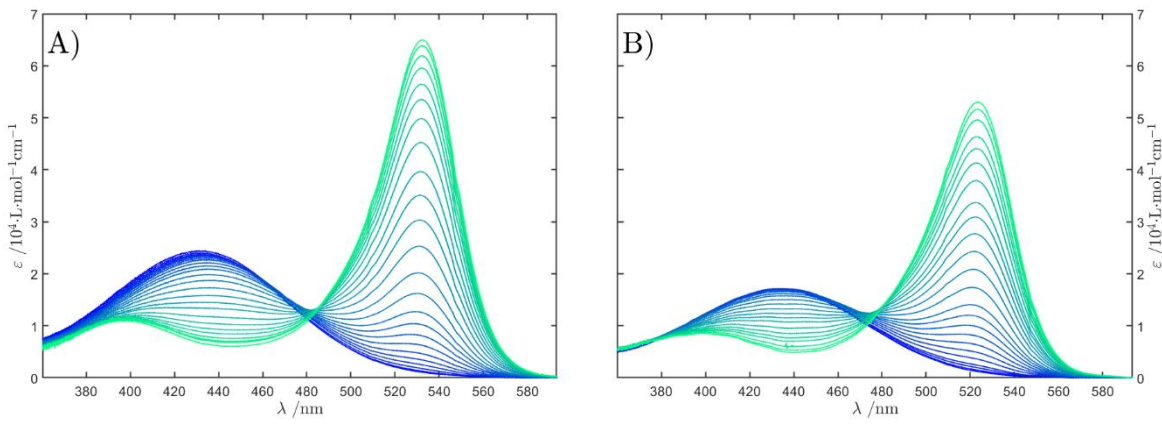


Figure S1: Spectra of BCP (A) and CPR (B) during the titration. The titration proceeded from the acidic-form ($\lambda_{\max} = 527 \text{ nm}$ and $\lambda_{\max} = 517 \text{ nm}$ for BCP and CPR, respectively) coded in green to the basic B-form ($\lambda_{\max} = 431 \text{ nm}$ and $\lambda_{\max} = 435 \text{ nm}$ for BCP and CPR, respectively) coded in blue.

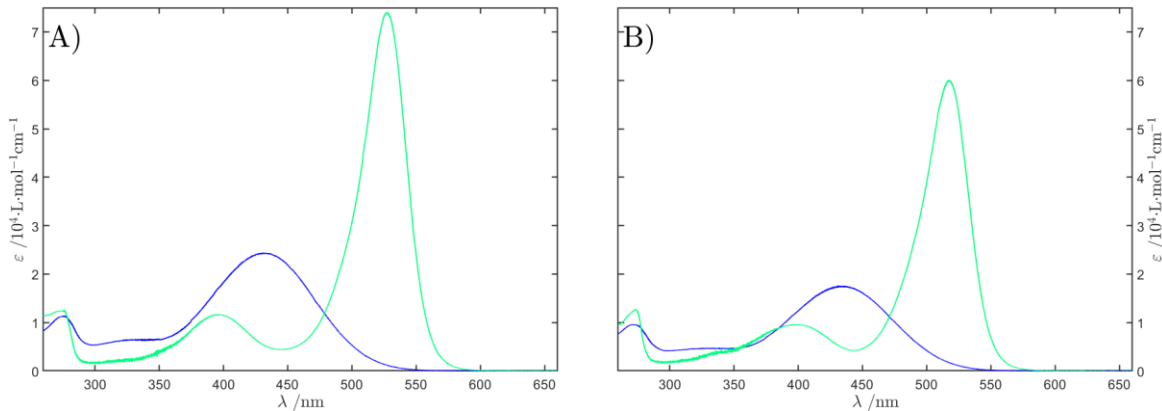


Figure S2: A) Spectra of pure forms of BCP's acidic A-form (green) and basic neutral B-form (blue). B) Spectra of pure spectral forms of CPR's acidic A-form (green) and basic neutral B-form (blue).

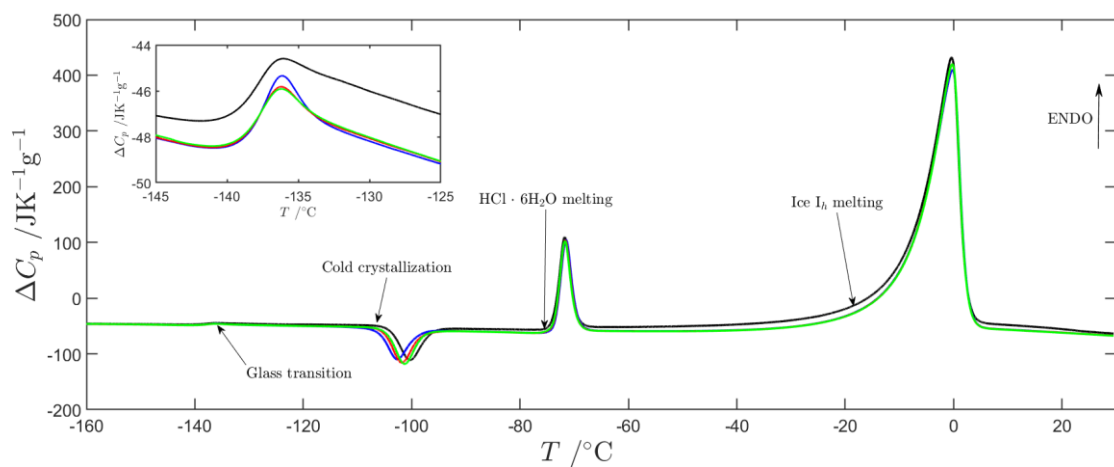


Figure S3: The full-ranged thermograms of 1 HCl sample showing the temperatures of $-160 \text{ }^{\circ}\text{C}$ to $30 \text{ }^{\circ}\text{C}$. All the features are signified by the arrow: the glass transition, cold crystallization, hydrochloric acid hexahydrate melting, and ice melting. The inset shows the magnification of glass transition in the range of $-145 \text{ }^{\circ}\text{C}$ to $-125 \text{ }^{\circ}\text{C}$.

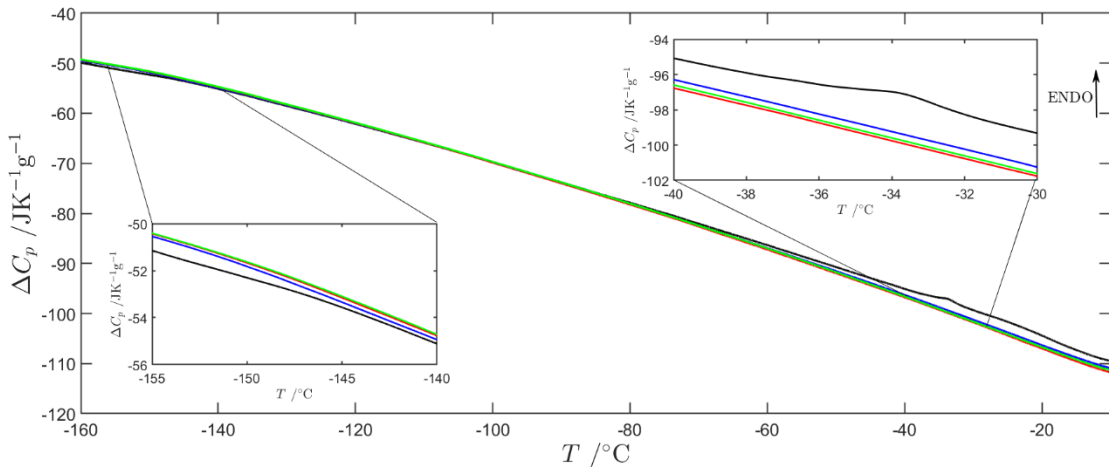


Figure S4: A thermogram of 10 mM HCl ($m = 10 \mu\text{g}$) in the relevant temperature range of -160°C to -30°C , the black line signifies cold loaded sample (frozen outside the DSC in liquid nitrogen). The blue, green and red lines show heating scans ($30^\circ\text{C}\cdot\text{min}^{-1}$) of samples cooled by the rate $30^\circ\text{C}\cdot\text{min}^{-1}$. The first inset ($T = <-155^\circ\text{C}, -140^\circ\text{C}>$) plot shows a magnification of the glass transition and the second inset ($T = <-40^\circ\text{C}, -30^\circ\text{C}>$) shows melting peak with an onset at -35°C in greater detail.

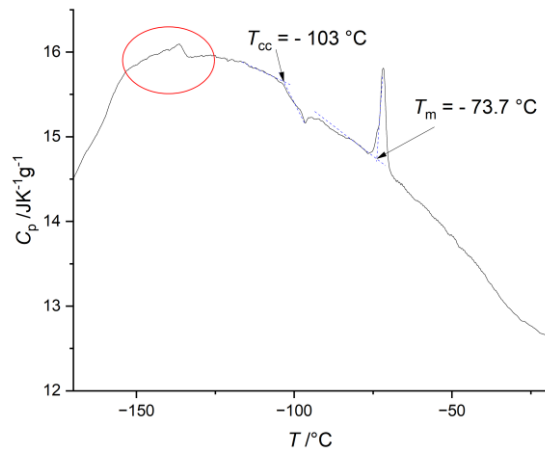


Figure S5: DSC scan of 10 mM HCl solution (sample weight $m = 50 \mu\text{g}$), the temperatures of cold crystallization (T_{cc}) and melting (T_m) are depicted. The red circle draws attention to the glass transition.

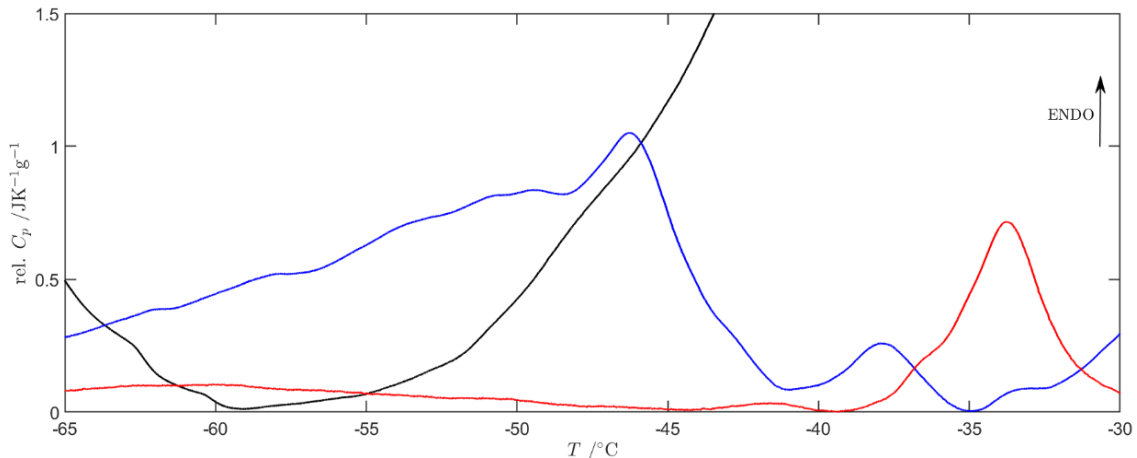


Figure S6: The selected parts of the thermograms of cold-loaded samples of HCl with initial concentrations of 1M (black), 100 mM (blue) and 10 mM (red) after subtraction of a straight lines to enhance the visibility of the peaks, which is why the thermal capacity is labeled as relative. Furthermore, constants were subtracted to show all of the thermographs at the same level.

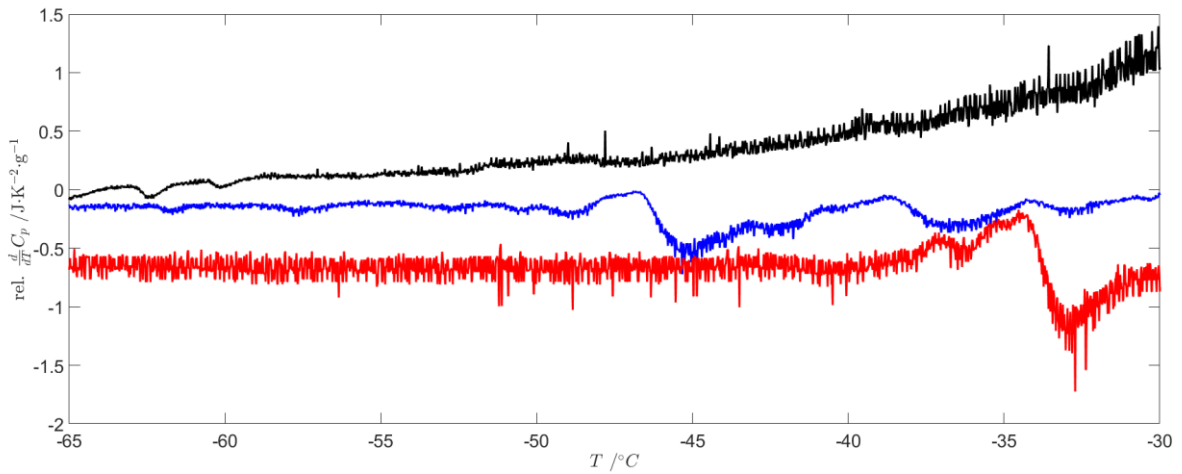


Figure S7: The first derivative of thermal capacity with respect to temperature for cold-loaded sample of 1M (black), 100 mM (blue), 10 mM (red) of HCl (depicted in Figure S6). The derivative is labeled as relative, because a constant was subtracted from the data to enhance visibility of the respective derivatives.

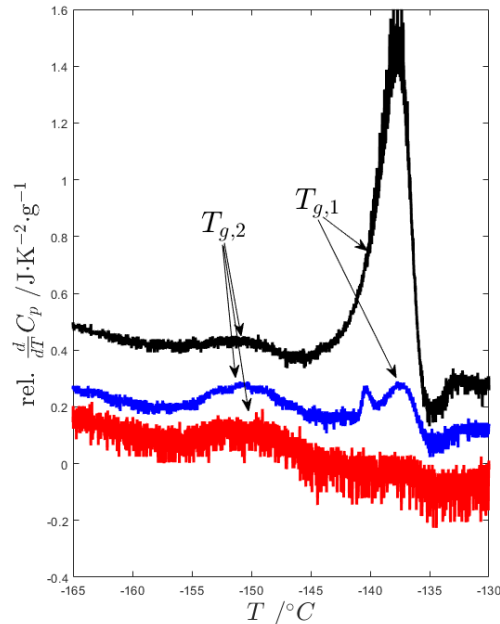


Figure S8: The first derivative of thermal capacity with respect to temperature for cold loaded sample of 1 M HCl(black), 100 mM (blue) and 10 mM (red) HCl sample. Both glass transitions are depicted with arrows. The ordinate is described as relative derivative because constants were subtracted from the derivatives to enhance the visibility of each glass transition.

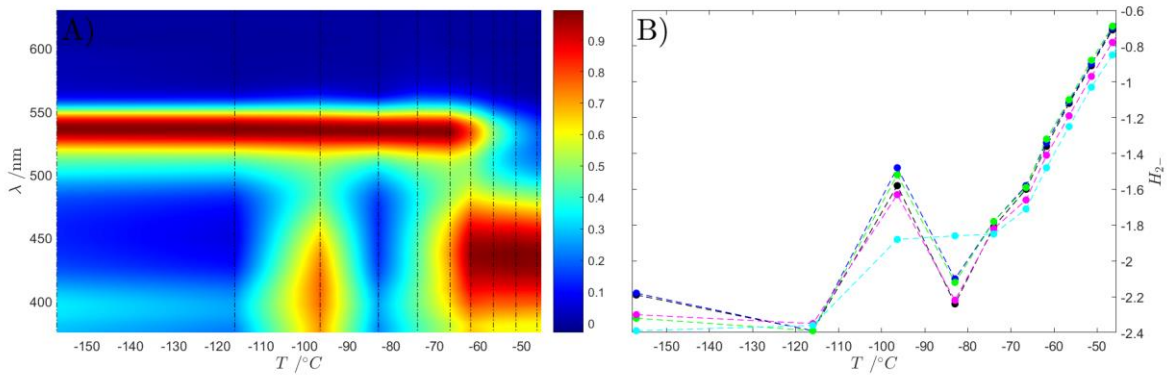


Figure S9: A) Dependence of selected BCP spectra on temperature for 500 mM HCl left to heat up from -196 °C to room temperature. The colorbar shows the normalized absorption of the averaged spectra. B) Dependence of Hammett acidity of 500 mM HCl frozen solution, each run of the experiment is plotted in different color.

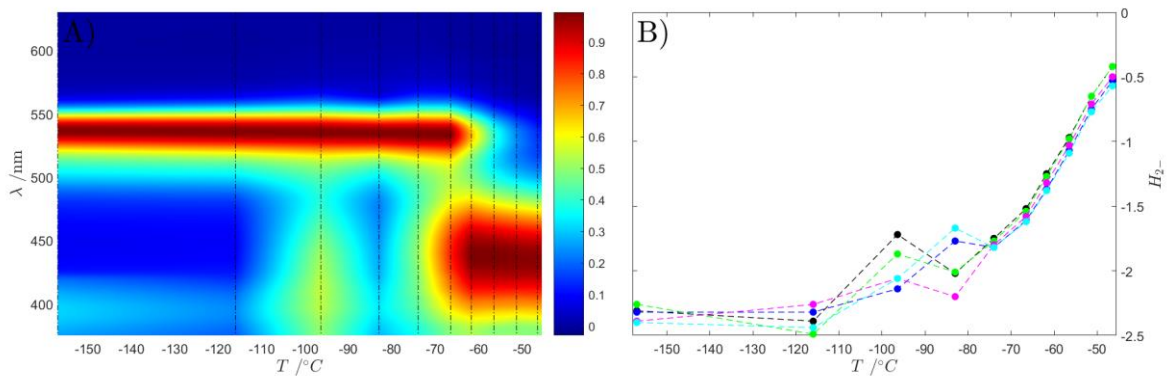


Figure S10: A) Dependence of selected BCP spectra on temperature for 200 mM HCl left to heat up from -196 °C to room temperature. The colorbar shows the normalized absorption of the averaged spectra. B) Dependence of Hammett acidity of 200 mM HCl frozen solution, each run of the experiment is plotted in different color.

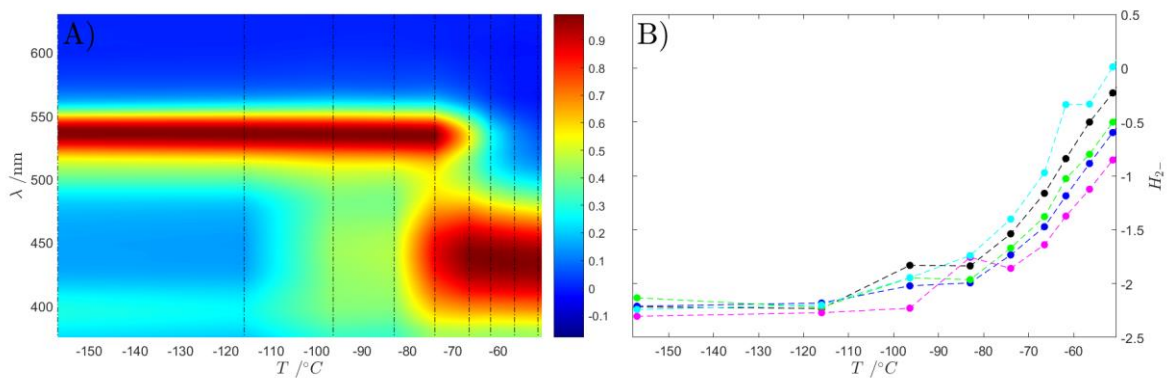


Figure S11: A) Dependence of selected BCP spectra on temperature for 50 mM HCl left to heat up from -196 °C to room temperature. The colorbar shows the normalized absorption of the averaged spectra. B) Dependence of Hammett acidity of 50 mM HCl frozen solution, each run of the experiment is plotted in different color.

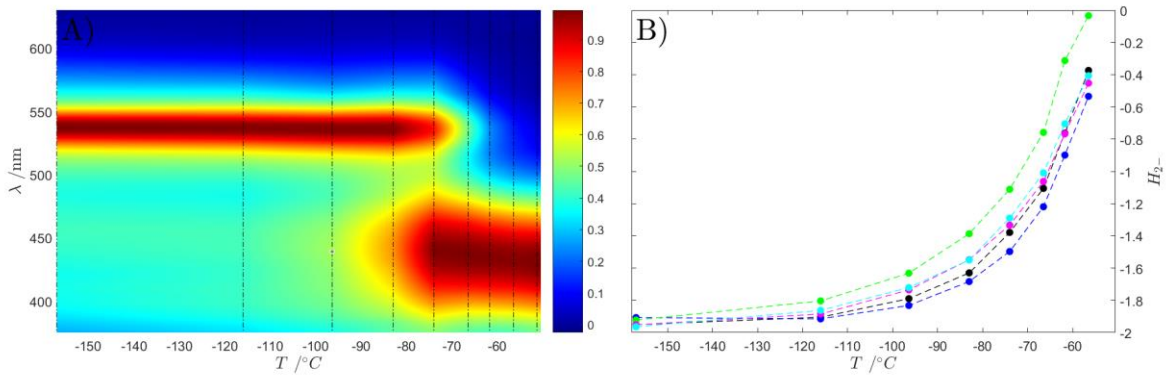


Figure S12: A) Dependence of selected BCP spectra on temperature for 10 mM HCl left to heat up from -196 $^{\circ}\text{C}$ to room temperature. The colorbar shows the normalized absorption of the averaged spectra. B) Dependence of Hammett acidity of 10 mM HCl frozen solution, each run of the experiment is plotted in different color.

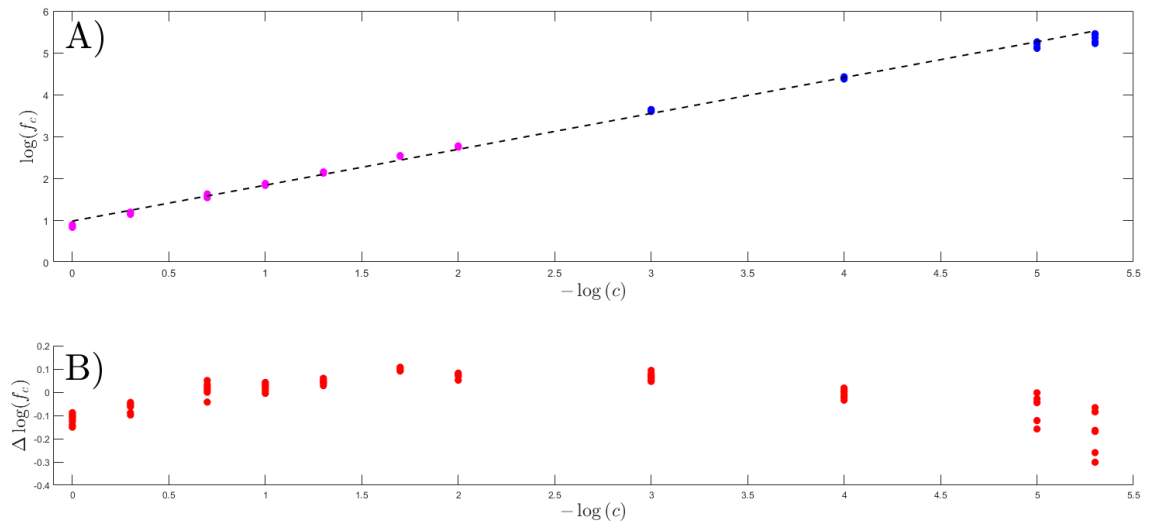


Figure S13: A) Dependence of decadic logarithm of concentration factor f_c on the negative decadic logarithm of initial HCl concentration. The magenta points show samples measured with BCP, whereas the blue points show samples measured with CPR (at $-\log(c) = 3$ both CPR and BCP points are present, they however overlap). The black line shows a linear fit of all the data points. B) The difference between the fitted line and the calculated f_c depicted in red with zero-line shown in black.

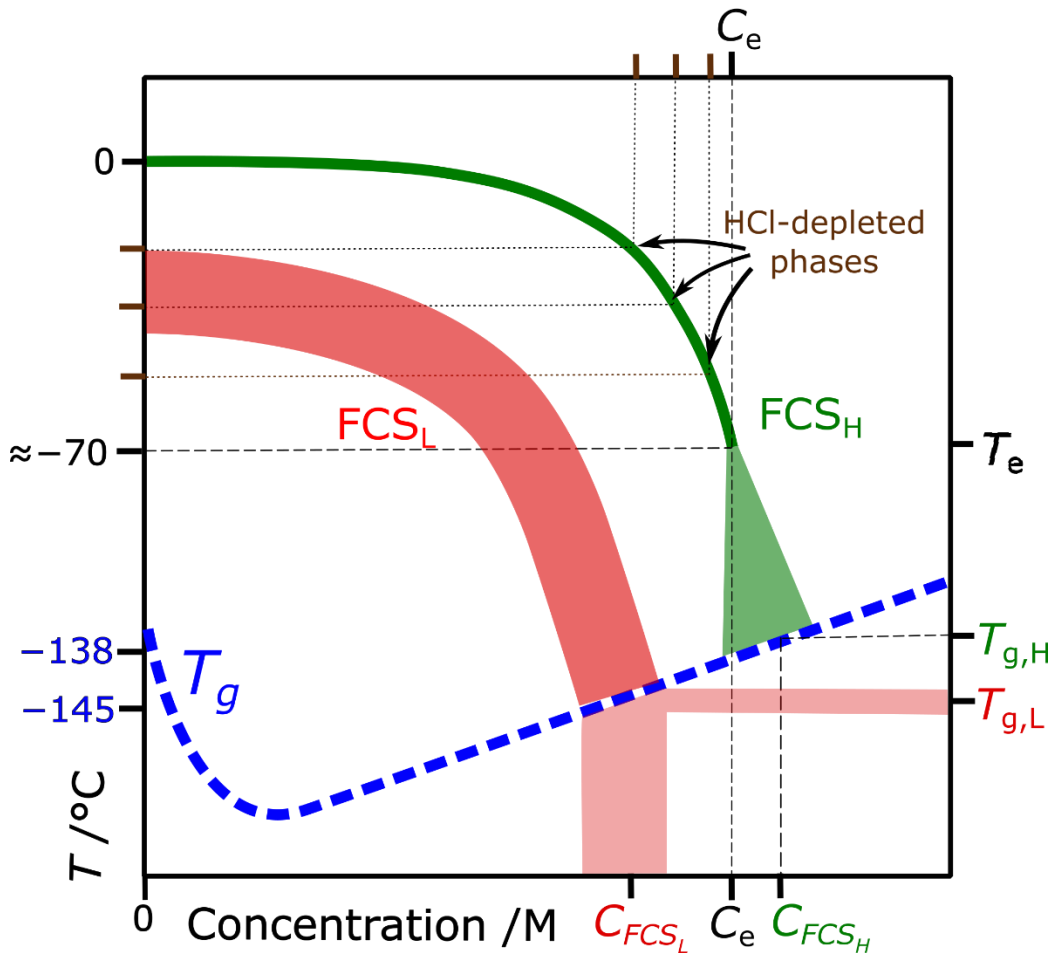


Figure S14: Schematic representation of the thermal behavior of HCl-H₂O system. The green line represents the liquidus line, the red line represents the supercooled aqueous solution's homogeneous crystallization temperature. The blue dashed line represents the T_g of aqueous solution with the characteristic minimum. The T_e and c_e are the eutectic temperature and concentration, respectively. The green line represents the scenario of FCS_H production, whereas the red shows the FCS_L, having lower solute concentration and lower glass transition temperature compared to the FCS_H.

Table S1: The enthalpies of cold crystallization (CC) and melting for the samples of 1000 mM, 100 mM and 10 mM HCl. The enthalpies correspond to the cold-loaded sample, and the three repetitions of cooling and subsequent heating both with a rate of 30 K/min in this order. The table is adorned with the average enthalpy and standard error of the mean (SEM). The enthalpies were obtained by integration, the relative error of which is typically less than 3 % for such kind of instruments after calibration¹. The exact same was found also for the calorimeter used here in previous work for typical cold-crystallization exotherms of 1300 J/mol ², and even for very weak thermal signal of less than 40 J/mol the error bar is no more than 2 J/mol ³.

<i>c</i> /mM	1000		100		10	
Type	CC	Melting	CC	Melting	CC	Melting
<i>H</i>	-957.74	1441.88	-117.15	163.70	-1.56	2.96
<i>H</i>	-875.47	1470.70	-94.03	147.50	.	.
<i>H</i>	-938.21	1451.86	-110.10	150.90	.	.
<i>H</i>	-951.10	1440.43	-107.68	151.34	.	.
\bar{H}	-930.63	1451.22	-107.24	153.36	.	.
SEM	18.83	6.97	4.84	3.55	.	.

Table S2: Table of sample's Hammett acidities of variously concentrated HCl samples ($1\text{ M} - 5 \cdot 10^{-6}\text{ M}$) depending on temperatures, which are shown as an interval. The indicators used are color-coded with BCP being magenta and CPR yellow. The individual errors are less than ± 0.2 , as estimated for this kind of analysis in a previous publication⁴.

$c = 1\text{ M}$						$c = 0.5\text{ M}$					
$\langle T_{\text{low}}, T_{\text{up}} \rangle /^\circ\text{C}$	H_{2^-}	H_{2^-}	H_{2^-}	H_{2^-}	H_{2^-}	$\langle T_{\text{low}}, T_{\text{up}} \rangle /^\circ\text{C}$	H_{2^-}	H_{2^-}	H_{2^-}	H_{2^-}	H_{2^-}
<-196, -131>	-2.56	-2.53	-2.49	-2.64	-2.43	<-196, -131>	-2.46	-2.18	-2.32	-2.30	-2.39
<-131, -105>	-2.58	-2.64	-2.72	-2.59	-2.57	<-131, -105>	-2.73	-2.39	-2.39	-2.35	-2.36
<-105, -88>	-2.69	-2.41	-2.60	-2.61	-2.49	<-105, -88>	-1.76	-1.48	-1.52	-1.63	-1.88
<-88, -77>	-2.38	-2.19	-2.32	-2.37	-2.15	<-88, -77>	-2.55	-2.10	-2.12	-2.22	-1.86
<-77, -70>	-2.15	-1.97	-2.18	-2.21	-2.03	<-77, -70>	-2.03	-1.78	-1.78	-1.82	-1.85
<-70, -64>	-1.92	-1.74	-1.99	-2.00	-1.97	<-70, -64>	-1.8	-1.72	-1.54	-1.79	-1.80
<-64, -59>	-1.69	-1.52	-1.80	-1.82	-1.82	<-64, -59>	-1.56	-1.49	-1.32	-1.60	-1.62
<-59, -54>	-1.46	-1.30	-1.61	-1.62	-1.63	<-59, -54>	-1.32	-1.26	-1.10	-1.41	-1.42
<-54, -49>	-1.24	-1.09	-1.42	-1.42	-1.45	<-54, -49>	-1.11	-1.04	-0.89	-1.22	-1.22
<-49, -44>	-1.04	-0.90	-1.24	-1.24	-1.27	<-49, -44>	-0.91	-0.84	-0.70	-1.04	-1.04
<-44, -40>	-0.88	-0.72	-1.07	-1.07	-1.10	<-44, -40>	-0.74	-0.68	-0.52	-0.87	-0.87
<-40, -36>	-0.69	-0.52	-0.91	-0.92	-0.92	<-40, -36>	-0.62	-0.49	-0.32	-0.71	-0.72
$c = 0.2\text{ M}$						$c = 0.1\text{ M}$					
$\langle T_{\text{low}}, T_{\text{up}} \rangle /^\circ\text{C}$	H_{2^-}	H_{2^-}	H_{2^-}	H_{2^-}	H_{2^-}	$\langle T_{\text{low}}, T_{\text{up}} \rangle /^\circ\text{C}$	H_{2^-}	H_{2^-}	H_{2^-}	H_{2^-}	H_{2^-}
<-196, -131>	-2.31	-2.32	-2.26	-2.39	-2.40	<-196, -131>	-2.36	-2.26	-2.35	-2.44	-2.35
<-131, -105>	-2.39	-2.32	-2.49	-2.26	-2.44	<-131, -105>	-2.44	-2.45	-2.44	-2.39	-2.39
<-105, -88>	-1.72	-2.14	-1.87	-2.06	-2.06	<-105, -88>	-2.19	-1.80	-1.81	-2.40	-2.28
<-88, -77>	-2.02	-1.77	-2.01	-2.20	-1.67	<-88, -77>	-2.10	-1.95	-1.88	-1.70	-1.84
<-77, -70>	-1.75	-1.82	-1.77	-1.80	-1.82	<-77, -70>	-1.89	-1.72	-1.62	-1.92	-1.90
<-70, -64>	-1.52	-1.61	-1.54	-1.58	-1.62	<-70, -64>	-1.66	-1.43	-1.32	-1.70	-1.70
<-64, -59>	-1.25	-1.37	-1.27	-1.32	-1.38	<-64, -59>	-1.40	-1.11	-0.97	-1.44	-1.46
<-59, -54>	-0.97	-1.07	-0.98	-1.03	-1.09	<-59, -54>	-1.19	-0.92	-0.81	-1.22	-1.25
<-54, -49>	-0.65	-0.75	-0.65	-0.71	-0.77	<-54, -49>	-0.96	-0.67	-0.58	-0.98	-1.02
<-49, -44>	-0.42	-0.53	-0.42	-0.50	-0.57	<-49, -44>	-0.76	-0.46	-0.42	-0.76	-0.78
<-44, -40>	-0.32	-0.44	-0.31	-0.39	-0.45	<-44, -40>	-0.55	-0.24	-0.20	-0.58	-0.60
<-40, -36>	-0.10	-0.24	-0.09	-0.17	-0.24	<-40, -36>	-0.42	-0.08	-0.19	-0.41	-0.40
$c = 5 \cdot 10^{-2}\text{ M}$						$c = 2 \cdot 10^{-2}\text{ M}$					
$\langle T_{\text{low}}, T_{\text{up}} \rangle /^\circ\text{C}$	H_{2^-}	H_{2^-}	H_{2^-}	H_{2^-}	H_{2^-}	$\langle T_{\text{low}}, T_{\text{up}} \rangle /^\circ\text{C}$	H_{2^-}	H_{2^-}	H_{2^-}	H_{2^-}	H_{2^-}
<-196, -131>	-2.22	-2.2	-2.13	-2.3	-2.24	<-196, -131>	-2.24	-2.19	-2.2	-2.2	.
<-131, -105>	-2.23	-2.2	-2.22	-2.27	-2.2	<-131, -105>	-2.26	-2.24	-2.3	-2.3	.
<-105, -88>	-1.83	-2	-1.95	-2.23	-1.95	<-105, -88>	-2.06	-1.82	-1.9	-1.9	.
<-88, -77>	-1.84	-2	-1.96	-1.76	-1.74	<-88, -77>	-2.03	-1.8	-1.9	-1.9	.
<-77, -70>	-1.54	-1.7	-1.67	-1.86	-1.4	<-77, -70>	-1.76	-1.51	-1.6	-1.7	.
<-70, -64>	-1.16	-1.5	-1.38	-1.64	-0.97	<-70, -64>	-1.51	-1.16	-1.4	-1.4	.
<-64, -59>	-0.84	-1.2	-1.03	-1.37	-0.34	<-64, -59>	-1.26	-0.87	-1.1	-1.2	.
<-59, -54>	-0.5	-0.9	-0.8	-1.13	-0.33	<-59, -54>	-1	-0.56	-0.8	-0.9	.
<-54, -49>	-0.23	-0.6	-0.5	-0.85	0.012	<-54, -49>	-0.75	-0.3	-0.5	-0.6	.
<-49, -44>	0.102	-0.3	-0.24	-0.6	0.403	<-49, -44>	-0.51	-0.01	-0.3	-0.4	.
$c = 1 \cdot 10^{-2}\text{ M}$						$c = 1 \cdot 10^{-3}\text{ M}$					

$\langle T_{\text{low}}, T_{\text{up}} \rangle / ^\circ\text{C}$	H_{2^-}	H_{2^-}	H_{2^-}	H_{2^-}	H_{2^-}	$\langle T_{\text{low}}, T_{\text{up}} \rangle / ^\circ\text{C}$	H_{2^-}	H_{2^-}	H_{2^-}	H_{2^-}	H_{2^-}
<-196, -131>	-1.95	-1.91	-1.92	-1.95	-1.96	<-196, -131>	-1.48	-1.51	-1.48	-1.48	-1.53
<-131, -105>	-1.90	-1.92	-1.80	-1.88	-1.86	<-131, -105>	-1.49	-1.48	-1.46	-1.49	-1.51
<-105, -88>	-1.79	-1.83	-1.63	-1.74	-1.72	<-105, -88>	-1.47	-1.44	-1.42	-1.47	-1.49
<-88, -77>	-1.63	-1.68	-1.39	-1.55	-1.55	<-88, -77>	-1.42	-1.37	-1.34	-1.42	-1.43
<-77, -70>	-1.38	-1.50	-1.11	-1.33	-1.29	<-77, -70>	-1.35	-1.21	-1.15	-1.34	-1.36
<-70, -64>	-1.11	-1.22	-0.76	-1.06	-1.01	<-70, -64>	-1.23	-0.96	-0.90	-1.18	-1.20
<-64, -59>	-0.76	-0.90	-0.31	-0.77	-0.71	<-64, -59>	-1.03	-0.67	-0.62	-0.97	-0.99
<-59, -54>	-0.37	-0.53	-0.03	-0.45	-0.41	<-59, -54>	-0.83	-0.34	-0.16	-0.77	-0.77
$c = 1 \cdot 10^{-3} \text{ M}$						$c = 1 \cdot 10^{-4} \text{ M}$					
$\langle T_{\text{low}}, T_{\text{up}} \rangle / ^\circ\text{C}$	H_{2^-}	H_{2^-}	H_{2^-}	H_{2^-}	H_{2^-}	$\langle T_{\text{low}}, T_{\text{up}} \rangle / ^\circ\text{C}$	H_{2^-}	H_{2^-}	H_{2^-}	H_{2^-}	H_{2^-}
<-196, -131>	-1.42	-1.46	-1.49	.	.	<-196, -131>	-0.86	-0.87	-1.07	-0.88	-0.89
<-131, -105>	-1.43	-1.50	-1.57	.	.	<-131, -105>	-0.83	-0.90	-1.06	-0.86	-0.90
<-105, -88>	-1.31	-1.42	-1.42	.	.	<-105, -88>	-0.87	-0.92	-1.02	-0.85	-0.88
<-88, -77>	-1.29	-1.38	-1.38	.	.	<-88, -77>	-0.89	-0.93	-1.01	-0.84	-0.87
<-77, -70>	-1.22	-1.34	-1.32	.	.	<-77, -70>	-0.86	-0.90	-0.97	-0.83	-0.86
<-70, -64>	-1.06	-1.24	-1.18	.	.	<-70, -64>	-0.78	-0.83	-0.90	-0.80	-0.82
<-64, -59>	-0.84	-1.05	-0.99	.	.	<-64, -59>	-0.70	-0.77	-0.81	-0.76	-0.77
<-59, -54>	-0.61	-0.86	-0.79	.	.	<-59, -54>	-0.60	-0.69	-0.72	-0.70	-0.71
$c = 1 \cdot 10^{-5} \text{ M}$						$c = 5 \cdot 10^{-6} \text{ M}$					
$\langle T_{\text{low}}, T_{\text{up}} \rangle / ^\circ\text{C}$	H_{2^-}	H_{2^-}	H_{2^-}	H_{2^-}	H_{2^-}	$\langle T_{\text{low}}, T_{\text{up}} \rangle / ^\circ\text{C}$	H_{2^-}	H_{2^-}	H_{2^-}	H_{2^-}	H_{2^-}
<-196, -131>	-0.61	-0.54	-0.40	.	.	<-196, -131>	-0.13	-0.42	-0.27	.	.
<-131, -105>	-0.56	-0.53	-0.35	.	.	<-131, -105>	-0.08	-0.39	-0.26	.	.
<-105, -88>	-0.55	-0.52	-0.39	.	.	<-105, -88>	-0.09	-0.40	-0.26	.	.
<-88, -77>	-0.55	-0.53	-0.41	.	.	<-88, -77>	-0.10	-0.40	-0.27	.	.
<-77, -70>	-0.53	-0.50	-0.39	.	.	<-77, -70>	-0.03	-0.35	-0.24	.	.
<-70, -64>	-0.49	-0.47	-0.32	.	.	<-70, -64>	0.03	-0.30	-0.17	.	.
<-64, -59>	-0.44	-0.43	-0.22	.	.	<-64, -59>	0.13	-0.23	-0.12	.	.
<-59, -54>	-0.38	-0.37	-0.11	.	.	<-59, -54>	0.26	-0.13	-0.03	.	.

Table S3: The Hammett acidity values at -150 °C and -115°C for each concentration with the indicator denoted as BCP or CPR. The Hammett acidities were used to calculate the concentration factor. The Table also includes the averages (\bar{H}_{2-}) and standard error of the mean (SEM). As mentioned in the caption of Table S2, the upper boundary of the errors is approx. ± 0.2 . The SEM calculated from the data is in all cases even lower than this upper boundary.

Indicator	c /M	H_{2-}				\bar{H}_{2-}	SEM	
BCP	1.00E+00	-2.56	-2.53	-2.49	-2.64	-2.43	-2.57	0.08
		-2.58	-2.64	-2.72	-2.59	-2.57		
BCP	5.00E-01	-2.19	-2.18	-2.32	-2.30	-2.39	-2.33	0.08
		-2.39	-2.39	-2.39	-2.35	-2.36		
BCP	2.00E-01	-2.31	-2.32	-2.26	-2.39	-2.40	-2.36	0.08
		-2.39	-2.32	-2.49	-2.26	-2.44		
BCP	1.00E-01	-2.36	-2.26	-2.35	-2.44	-2.35	-2.39	0.06
		-2.44	-2.45	-2.44	-2.39	-2.39		
BCP	5.00E-02	-2.22	-2.21	-2.13	-2.30	-2.24	-2.22	0.05
		-2.23	-2.18	-2.22	-2.27	-2.20		
BCP	2.00E-02	-2.24	-2.19	-2.21	-2.17	.	-2.23	0.04
		-2.26	-2.24	-2.26	-2.26	.		
BCP	1.00E-02	-1.95	-1.91	-1.92	-1.95	-1.96	-1.91	0.05
		-1.90	-1.92	-1.80	-1.88	-1.86		
BCP	1.00E-03	-1.48	-1.51	-1.48	-1.48	-1.53	-1.49	0.02
		-1.49	-1.48	-1.46	-1.49	-1.51		
CPR	1.00E-03	-1.42	-1.46	-1.49	.	.	-1.48	0.06
		-1.43	-1.50	-1.57	.	.		
CPR	1.00E-04	-0.86	-0.93	-0.87	-0.88	-0.89	-0.89	0.04
		-0.83	-0.95	-0.90	-0.86	-0.90		
CPR	1.00E-05	-0.61	-0.54	-0.40	.	.	-0.50	0.10
		-0.56	-0.53	-0.35	.	.		
CPR	5.00E-06	-0.13	-0.42	-0.27	.	.	-0.26	0.14
		-0.08	-0.39	-0.26	.	.		

Script S1: The script is a MatLab function that takes in a vector of Hammett acidities as an input and returns the vector of corresponding concentrations as an output. Furthermore, it returns the control figure which shows the blue plot of the whole dependence of Hammett acidity on concentration and the input Hammett acidity with resulting concentration as a black scatter.

```

function [vec_out] = recalculate_H_to_c(vec_in)
%Recalculates a given input vector (Hammett acidity) into an output
%variable of concentration
    %Call the function like this: result = recalculate_H_to_c(Hammett_vector)

%Coefficients of the pseudo-polynomials used in the calculation
coeff_H_on_w = [2.192e-9 -1.932e-7 5.681e-6 -5.720e-5 -1.184e-3 -4.164e-2 5.474e-1 -4.450e-1];
coeff_c_on_w = [-2.907e-10 1.877e-8 -4.472e-7 7.214e-6 1.274e-3 2.737e-1 0.000 0.000];

%Create a weight percentage vector
w = 0.0001:0.0001:36;

%Calculate the Hammett acidity and the concentration
H = coeff_H_on_w(end)*log(w) + coeff_H_on_w(end-1)*w + coeff_H_on_w(end-2)*w.^2 + coeff_H_on_w(end-3)*w.^3 + coeff_H_on_w(end-4)*w.^4 + coeff_H_on_w(end-5)*w.^5 + coeff_H_on_w(end-6)*w.^6;
c = coeff_c_on_w(end)*log(w) + coeff_c_on_w(end-1)*w + coeff_c_on_w(end-2)*w.^2 + coeff_c_on_w(end-3)*w.^3 + coeff_c_on_w(end-4)*w.^4 + coeff_c_on_w(end-5)*w.^5 + coeff_c_on_w(end-6)*w.^6;

%Cubic spline interpolation is used to determine the precise concentration
%from the given Hammett acidity
vec_out = spline(H,c,vec_in);

%Creation of control plot
fig1 = figure("Name","Control plot", "Position", [.25 .25 1080 640]);
ax1 = axes("Position", [0.1 0.1 0.85 0.85], "FontSize", 16, "LineWidth", 2);
box(ax1, "on")
hold(ax1, "on")

plot(ax1,c,H, "LineWidth", 2.5, "Color", "b")
scatter(vec_out, vec_in, 75, "k", "filled")

xlabel(ax1, "$c$ / M", "FontSize", 18, "Interpreter", "latex", "FontWeight", "bold")
ylabel(ax1, "$H$ ^s", "FontSize", 18, "Interpreter", "latex", "FontWeight", "bold")

end

```

References

1. Hemminger, W. F.; Sarge, S. M., The Baseline Construction and Its Influence on the Measurement of Heat with Differential Scanning Calorimeters. *Journal of thermal analysis* **1991**, *37*, 1455-1477.
2. Elsaesser, M. S.; Winkel, K.; Mayer, E.; Loerting, T., Reversibility and Isotope Effect of the Calorimetric Glass → Liquid Transition of Low-Density Amorphous Ice. *Physical Chemistry Chemical Physics* **2010**, *12*, 708-712.
3. Tonauer, C. M.; Yamashita, K.; Rosso, L. d.; Celli, M.; Loerting, T., Enthalpy Change from Pure Cubic Ice Ic to Hexagonal Ice Ih. *The Journal of Physical Chemistry Letters* **2023**, *14*, 5055-5060.
4. Veselý, L.; Štůsek, R.; Mikula, O.; Yang, X.; Heger, D., Freezing-Induced Acidification of Sea Ice Brine. *Science of The Total Environment* **2024**, *946*, 174194.
5. Baskaran, A.; Kaari, M.; Venugopal, G.; Manikkam, R.; Joseph, J.; Bhaskar, P. V., Anti Freeze Proteins (Afp): Properties, Sources and Applications - a Review. *Int J Biol Macromol* **2021**, *189*, 292-305.